A Numerical Study of Premixed Flames Darrieus-Landau Instability

B. Denet[a]; P. Haldenwang[a]

[a] Laboratoire de Recherche en Combustion, Université de Provence-Centre de Saint Jérome (S 252), Marseille, Cedex 20, France

PLEASE SCROLL DOWN FOR ARTICLE

A Numerical Study of Premixed Flames Darrieus-Landau Instability

B. DENET and P. HALDENWANG *Laboratoire de Recherche en Combustion, Université de Provence-Centre de Saint Jérôme (S 252), 13397 Marseille Cedex 20, France*

ABSTRACT—The complete equations of premixed flames are solved numerically, in the isobaric approximation and with a simplified chemical kinetics. A momentum-pressure formulation is proposed for solving non-constant density flows. The growth rates of the Darrieus-Landau instability are measured and compared to the linear theory. Large amplitude curved flames are obtained, as well as flames submitted to a shear flow.

Key Words: Darrieus-Landau instability, variable density flows, numerical combustion, flame dynamics, curved flames

1 INTRODUCTION

The instability of plane premixed flames propagating in tubes, leading to wrinkled flames, has been the subject of various works; for reviews see Sivashinsky (1983), Williams (1985) and Clavin (1985). Two major explanations of this phenomenon exist. The first one is the thermal-diffusive instability: the main cause of the instability is the diffusion of limiting species. The second source of wrinkling is the Darrieus-Landau instability: in this case, the cause of instability is the density jump at the flame front, leading to a deflection of streamlines. In a previous paper (Denet and Haldenwang, 1992), we focused our interest on the thermal diffusive instability, which is a consequence of diffusive effects through the thickness of the flame. This instability was exhibited in a simplified model neglecting density changes in the flow (see Barenblatt *et al.*, 1962).

In this paper, on the contrary, we are interested in the Darrieus-Landau instability, which requires to solve the complete set of Navier Stokes equations. In the first historical studies of this hydrodynamic instability, only the destabilizing influence of density changes across the flame was taken into account (see Darrieus, 1938; Landau, 1944). Later studies showed the influence of diffusion and gravity as stabilizing effects on this instability (see Pelcé and Clavin, 1982). On the contrary, the effect of viscosity seemed to be quite negligible, at least in the linear domain. Corroborating results were obtained by Matalon and Matkowsky (1982) and by Frankel and Sivashinsky (1983). All these papers are theoretical works, using asymptotic and multi-scale methods to reduce the study of reaction and flame zones to jump conditions. Experimental results were reported in Quinard *et al.* (1984). The work of Jackson and Kapila (1984) used a mixed numerical-theoretical method: jump conditions were prescribed on the

reaction zone, the linearized equations outside this zone being solved numerically. In this last paper, only the stability limits are given, and not values of growth rates.

Here, we use a complete numerical approach of this type of problems. In this study, we are essentially interested in computations of growth rates, and in obtaining curved solutions, produced by the Darrieus-Landau instability in the nonlinear regime. The problem of obtaining the stability limits will not be addressed here: actually it would result in a huge number of growth rates to be measured. The way that we have chosen to effectively test the theoretical predictions concerning the Darrieus-Landau instability is to numerically measure growth rates, for different physical parameters. The theoretical predictions are based on two different limits. The large activation energy limit used by activation energy asymptotics makes possible to isolate a small reaction zone inside the flame. Then the low wavenumber limit permits one to consider the whole flame as a discontinuity in the hydrodynamical problem. It is natural to expect that when both limits are satisfied, the theoretical growth rates will get very close to the values we will numerically measure, and this is in fact what happens, thus validating the numerical method. However, we will vary the physical parameters of the problem in realistic ranges, showing that in some cases the theoretical results deteriorate in an important way, mainly because of the low wavenumber assumption. Of course, these discrepancies will not invalidate the theoretical results, but just show some light on the range of applicability of the limits used in the asymptotics. In any case, there is a qualitative agreement between the theory and our results.

To our knowledge, the first curved flame, resulting from the Darrieus-Landau instability, was obtained by Spalding and Wu (1986), using a numerical method considering the flame as a discontinuity. The work presented here is an extension of a preliminary work (Denet, 1988), in which all the equations of the physical problem were solved, even in the reaction zone, but using simplifying assumptions, particularly on the viscosity term. A more complicated approach to this type of problems can be found in Fröhlich and Peyret (1991).

The set of hydrodynamical equations we have to solve here, is derived in the low Mach number limit (see for instance Majda and Sethian, 1985). In section 2, we recall these equations. In section 3, the linear theory results are presented, with the notations of Pelcé and Clavin (1982). Section 4 is concerned with the numerical scheme. Solving the isobaric, nonconstant density equations is a relatively difficult task: a classical problem arises from the estimate of the pressure field. In our present approach, because of the use of Fourier pseudo-spectral methods in the direction perpendicular to the flame velocity, we are faced with an additional specific difficulty. Section 5 presents a set of numerical results concerning the growth rates of the Darrieus-Landau instability. Comparison with theoretical predictions is included in this section. Finally, in section 6 we show typical steady nonlinear solutions.

2 BASIC EQUATIONS

Because the present simulation will lead to a large amount of computation, we choose the simplest chemistry: a single one-step chemical reaction is assumed. Non-dimensional quantities are obtained using a classical approach: the length scale is the flame

thickness obtained from asymptotics, likewise the velocity unit is the asymptotic flame speed. The use of normalized quantities allows us (see e.g. Clavin, 1985) to write the model, in a frame moving with the flame front, as follows:

$$\rho \frac{\partial T}{\partial t} + \rho (\vec{v} \cdot \vec{\nabla}) T = \Delta T + \Omega \tag{II.1a}$$

$$\rho \frac{\partial C}{\partial t} + \rho (\vec{v} \cdot \vec{\nabla}) C = \frac{1}{Le} \Delta C - \Omega \tag{II.1b}$$

with

$$\Omega = \frac{\beta^2}{2Le} C \frac{\rho}{1-\gamma} \exp\left(\frac{\beta(T-1)}{1+\gamma(T-1)}\right) \tag{II.2}$$

and

$$\frac{\partial (\rho)}{\partial t} + \vec{\nabla} \cdot (\rho \vec{v}) = 0 \tag{II.3a}$$

$$\frac{\partial (\rho \vec{v})}{\partial t} + \vec{\nabla} \cdot (\rho \vec{v} \vec{v}) = -\vec{\nabla} P + \rho \vec{G} + \mu \Delta \vec{v} + (\lambda + \mu/3) \vec{\nabla} (\vec{\nabla} \cdot \vec{v}) \tag{II.3b}$$

$$\rho = \left(1 + \frac{\gamma}{1-\gamma} T\right)^{-1} \tag{II.4}$$

where T and C correspond to the reduced temperature of the gas mixture and concentration of a reactant (the other reactant being in excess). The boundary conditions on T and C are

$$T(x = -\infty, y) = 0, \quad T(x = +\infty, y) = 1$$

$$C(x = -\infty, y) = 1, \quad C(x = +\infty, y) = 0$$

all quantities being periodic in the y direction (the direction transverse to the flame velocity).

$Le = D_{th}/D_{mol}$, $\beta = (E/R T_b^2)(T_b - T_u)$ and $\gamma = (T_b - T_u)/T_b$ are respectively the Lewis number of the reactant (ratio of thermal to molecular diffusivity), the reduced activation energy (or Zeldovich number) and the heat release parameter (T_b and T_u being respectively the temperature of burnt and unburnt gases, R is the constant of perfect gases). ρ, v, P are the density, velocity and pressure; G is an external specific force per unit volume (gravity for instance); μ and λ are respectively shear and bulk viscosities. Let us define U, the reduced flame speed which is an unknown of the problem. U is supposed to be parallel to the x-direction. G will also be parallel to this direction, positive and negative G corresponding respectively to downward and upward propagating flame (G being the inverse of the Froude number).

Among the various Equations II.1a and II.1b are the reaction-diffusion equations, II.3a and II.3b are the hydrodynamical equations; II.3a is the continuity equation, II.3b being the momentum Equations. II.4 is the perfect gas state equation, in the isobaric approximation. We will be interested in flames at very low Mach numbers, in an .open tube, where this approximation is indeed valid. Reaction-diffusion and

hydrodynamic equations are coupled through the density. As gas expansion across the flame front is important (we will often take as a typical value $\gamma = 0.8$, case where the burnt gas density is five times lower than the unburnt gas density) hydrodynamic effects have a large influence on the flame.

3 THEORETICAL RESULTS

Gas expansion generates deflection of streamlines across the curved flame front as a consequence of conservation of transverse velocity and of normal mass flux. Perturbation of the flow is thus produced by this deflection, on a scale of the order of the wavelength.

The linearized Darrieus-Landau analysis did consider only this destabilizing effect: the result was that the front was unstable at all wavelengths. Stabilizing effects, such as diffusion and gravity for downward propagating flames, were overlooked. A complete analytical theory, valid for low k, was obtained by Pelcé and Clavin (1982). In the sequel, we will explain the main points of this paper and give the theoretical formulas for growth rates of the Darrieus-Landau instability.

In this paper, the authors remark that the flame thickness d is generally smaller than the wavelength l of the perturbation. They introduce a small parameter $\varepsilon = d/l \ll 1$ and begin to develop the solution in powers of ε around the stationary plane flame. A multi-scale method is used to describe the spatial structure of the flow. The problem is thus split in two parts:

—a local study of the curved flame structure, submitted to an inhomogeneous upstream flow, considered as given in this first step (see Clavin and Williams, 1982). The study combines a multi-scale method ($\varepsilon \ll 1$) and an asymptotic method ($\beta \gg 1$).

—a nonlocal study of hydrodynamics, considering the flame as a discontinuity. The boundary conditions on the flame surface (jump conditions on pressure and velocity) are known as results of the previous local study.

A complete linearized analysis is thus obtained. Let us denote the growth rate and k the wavelength of the perturbation. An important parameter of the problem is the Markstein length L, defined in units of flame thickness, by

$$L = \frac{1}{\gamma}\ln\frac{1}{1-\gamma} + \frac{\beta(Le-1)}{2}\left(\frac{1-\gamma}{\gamma}\right)\int_0^{\gamma/(1-\gamma)}\frac{\ln(1+x)}{x}dx.$$

The final result is that there is an instability threshold, above which exists a band of unstable wave vectors, centered on

$$k_c = 2(1-\gamma)G$$

The dispersion relation reads

$$A(k)\sigma^2 + B(k)\sigma + C(k) = 0$$

with

$$A(k) = 2 - \gamma + \gamma \left(L - \frac{1}{\gamma} \ln \frac{1}{1-\gamma} \right) k$$

$$B(k) = 2k + \left(\frac{2}{1-\gamma} L - \frac{2}{1-\gamma} \ln \frac{1}{1-\gamma} \right) k^2$$

$$C(k) = \frac{\gamma}{1-\gamma} k \left(\frac{1}{2} k_c - k \left(\delta - \frac{k}{k^*} \right) \right)$$

where

$$\delta = 1 + G(1-\gamma) \left(L - \frac{1}{\gamma} \ln \frac{1}{1-\gamma} \right)$$

$$k^* = \left(1 + \frac{2+\gamma}{\gamma} L - \frac{2}{\gamma} \ln \frac{1}{1-\gamma} \right)^{-1}.$$

The stability limit is given by $C = dC/dk = 0$, the plane front being unstable for $C > 0$, which correspond to $k^* < 2k_c$.

We will recall the different hypotheses leading to this dispersion relation; first of all, we need $k \ll 1$ (the flame thickness must be small compared to the wavelength in order to use multi-scale analysis). Also, G must be of the order ε, which means that for non-vanishing G, k must not be too small compared to G. For vanishing G, the dispersion relation is actually valid only to terms of order k^2, the first term of this development giving exactly the Darrieus-Landau dispersion relation, i.e.

$$\sigma = \frac{k}{2-\gamma} \left(\sqrt{\frac{1+\gamma-\gamma^2}{1-\gamma}} - 1 \right).$$

The second term of this development can also be calculated in a straightforward way (it will be used in a forthcoming section):

$$\frac{k^2}{2-\gamma} \left\{ -L \frac{2-\gamma^2}{(1-\gamma)(2-\gamma)} + \ln \left(\frac{1}{1-\gamma} \right) \frac{3-2\gamma}{(1-\gamma)(2-\gamma)} \right.$$

$$\left. + \frac{1}{2} ((1-\gamma)(1+\gamma-\gamma^2))^{-1/2} \left[-\gamma(2-\gamma) + 2L(\gamma^2-1) + \ln \left(\frac{1}{1-\gamma} \right) (2-3\gamma) \right] \right\}.$$

There is an additional hypothesis worth mentioning: we need $\beta \gg 1$ in order to use jump conditions across the reaction zone (and for the dispersion relation to be valid). Although, in the case of the thermal-diffusive instability, it was difficult to satisfy this condition for typical values of β (see Denet and Haldenwang, 1992), we will see in the sequel that this restriction is less important in the case of the Darrieus-Landau instability.

Another important point about the Pelcé-Clavin dispersion relation is that, at leading orders in k, there is no dependency of the growth rates on the viscosities. We will see later that our numerical results agree with this prediction.

4   THE NUMERICAL METHOD

Our program makes use of Fourier series, in the y direction, and of finite differences, in the x direction. In the x direction, the mesh can be uniform or self-adaptive. There is also the possibility of using change of variables (always in the x direction) to locate more points in the reaction zone.

From the point of view of temporal discretization, the method is first order in time, the production term being taken explicitly, which limits the time step to low values, because of stability requirements. Convection terms are also explicit, but all diffusion terms are taken implicitly. When measuring growth rates of the diffusive-thermal instability (Denet and Haldenwang, 1992), we have not seen much differences between first and second order in time: the difference was of the order of 5% in the worst cases. The second order scheme being approximately twice as expensive as the first order one (the time step being further reduced), we have decided here to content ourselves with a first order scheme because, of course, computations are more expensive for the complete model, including the hydrodynamic equations, than those for only two reaction-diffusion equations.

We have now to give some explanations about the way we solve the Navier-Stokes equations, while satisfying the continuity equation. Recall that we adopt the isobaric approximation, valid for low Mach number flows. In this approximation, the pressure is no more considered as a thermodynamic quantity, and actually does not occur in the state equation, but as a dynamical quantity, chosen to satisfy the continuity equation. When density is constant (incompressible hydrodynamics) a common strategy to solve such problems is to solve a Poisson equation for pressure (see Roache, 1972). Our method is an extension of this technique for flows with variable density. Contrary to a previous version (Denet, 1988), our code is time-dependent and takes into account the viscosity term without approximation.

The second viscosity term, which reads

$$(\lambda + \mu/3)\vec{\nabla}(\vec{\nabla} \cdot \vec{v})$$

can be discarded because it can be incorporated in the pressure gradient (in the isobaric approximation) to define a new dynamical pressure. We have verified that discarding this term has no influence on the computation. Linan (1990) suggested that it might be possible to reduce the pressure jump across the flame by considering, instead of the second viscosity term

$$-\mu\vec{\nabla}(\vec{\nabla} \cdot \vec{v})$$

which defines as above a new dynamical pressure. Although it appears that the pressure jump is reduced, we have not seen any difference on the velocity field due to this modification. In our calculations we simply discard the second viscosity term.

Let us denote by Δt the value of the time step and by n, a superscript corresponding to quantities taken at the time $n\Delta t$. We begin by solving the thermal-diffusive equations on T and C divided by ρ. There is a numerical difficulty because we have variable diffusivities in space, proportional to $1/\rho$. To take implicitly these variable diffusion coefficients with a first order in time scheme while being unconditionally stable on these terms, we have to take implicitly at least half of the maximum of the diffusive term (see

Gottlieb et Orszag, 1977) leading to the following scheme:

$$\frac{1}{\Delta t} T^{n+1} = d\,\Delta T^{n+1} + S_T^n$$

$$\frac{1}{\Delta t} C^{n+1} = \frac{d}{Le}\Delta C^{n+1} + S_C^n$$

with

$$S_T^n = \frac{1}{\Delta t} T^n - (\vec{v}\cdot\vec{\nabla}) T^n + \left(\frac{1}{\rho^n} - d\right)\Delta T^n + \frac{\Omega^n}{\rho^n}$$

and

$$S_C^n = \frac{1}{\Delta t} C^n - (\vec{v}\cdot\vec{\nabla}) C^n + \frac{1}{Le}\left(\frac{1}{\rho^n} - d\right)\Delta C^n - \frac{\Omega^n}{\rho^n}$$

where $d = \alpha\max(1/\rho^n)$ with $\alpha\in[0.5;1]$ for a first order time discretization. The maximum is taken in the whole computational domain.

When T^{n+1} has been obtained from the previous equations, the value of ρ^{n+1} is deduced using the state equation, and the hydrodynamical equations are solved:

$$\frac{1}{\Delta t}(\rho\vec{v})^{n+1} = \mu d\,\Delta(\rho\vec{v})^{n+1} + \vec{S}_v^n - \vec{\nabla}P^{n+1}$$

with

$$\vec{S}_v^n = \frac{1}{\Delta t}(\rho\vec{v})^n - \vec{\nabla}\cdot(\rho\vec{v}\cdot\vec{v})^n + \mu(\Delta v^n - d\Delta(\rho\vec{v})^n) - \rho^{n+1}G$$

where P^{n+1} must be determined in order to satisfy the continuity equation at time $n + 1$. But before that, we will show that the discretization is stable on the diffusive term. This is not a priori obvious, because we have used the ρv variable (it will permit us to solve in an easier way the continuity equation) although the diffusive term is expressed in the v variable. We have to express the Laplacian of velocity in the ρv variable, giving the following formula:

$$\Delta\vec{v} = \frac{1}{\rho}\Delta(\rho\vec{v}) + 2\vec{\nabla}\left(\frac{1}{\rho}\right)\cdot\vec{\bar{\nabla}}(\rho\vec{v}) + \Delta\left(\frac{1}{\rho}\right)\rho\vec{v}.$$

In this formula, only the first term of the right hand side could limit seriously the time step if it was taken explicitly, because of the second derivative in ρv. This term is actually a diffusive term with variable coefficient and must be taken implicitly. We have seen previously that in order to take implicitly this type of term, at least half of the maximum diffusion term must be taken implicitly, which gives $\mu d\Delta(\rho v)$, where d has been previously defined. The rest of $\mu\Delta(v)$, i.e. $(\mu\Delta(v) - \mu d\Delta(\rho v))$, can be taken explicitly without any serious stability problem.

Now we have only to determine P^{n+1} such that the velocity at time $n + 1$ satisfies the continuity equation . It is obtained in taking the divergence of the previous time discretized Navier Stokes equation; using furthermore that ρv satisfies the discretized

continuity equation:

$$\frac{1}{\Delta t}\rho^{n+1} - \frac{1}{\Delta t}\rho^n + \vec{\nabla}\cdot(\rho\vec{v}) = 0$$

we obtain the following Poisson equation for pressure:

$$\Delta P^{n+1} = S_P$$

with

$$S_p = \vec{\nabla}\cdot\vec{S}_v^n + \left(\frac{1}{\Delta t} - \mu d\Delta\right)\left(\frac{1}{\Delta t}\rho^{n+1} - \frac{1}{\Delta t}\rho^n\right).$$

The same algorithm works also when a change of variable is used, thus modifying the spatial differential operators (see next section).

Let us now talk about the boundary conditions. We make our simulations in a bounded domain $[-X_0, X_0]*[-Y_0, Y_0]$. All quantities are periodic in the y direction. In the x direction, the following boundary condition are used in the numerical simulations

in $x = -X_0$ 　　　　　$T = 0$ 　$C = 1$ 　$\rho v_x = U$ 　$\rho v_y = 0$

in $x = X_0$ 　　　　　$\dfrac{\partial T}{\partial x} = 0$ 　$\dfrac{\partial C}{\partial x} = 0$ 　$\dfrac{\partial(\rho v_x)}{\partial x} = 0$ 　$\rho v_y = 0.$

In $x = X_0$, the boundary conditions on the velocities are compatible with the continuity equation. We have defined previously U, the flame velocity.

Finally, how do we succeed in keeping the flame in the computational domain? We define, at each time-step, the front position as the mean position of some temperature line. This flame position changes from one time-step to the next, thus defining a drift velocity δu. In order to keep the flame at the same position in the mean, we simply add at each time-step the drift velocity to the flame velocity U (thus modifying the boundary condition) and to the longitudinal velocity field v_x. We neglect the acceleration terms, due to this procedure, which are very small.

5 COMPUTATION OF GROWTH RATES OF THE DARRIEUS-LANDAU INSTABILITY

5.1 Numerical aspects

The techniques described in this section were used in our study of diffusive-thermal instability (Denet and Haldenwang, 1992). They can be adapted without any difficulty to the Darrieus-Landau instability.

For computing growth rates, we take as initial condition a sinusoidal flame of low amplitude (10^{-5} in units of flame thickness). After some transient, the amplitude begins to grow exponentially; we actually measure the growth rate of some norm (in the x direction) of the Fourier components of T (in the y direction) corresponding to the sine we have taken as initial condition. The results do not depend on the norm selected.

We take advantage of the fact that the sinusoidal flame is nearly plane to use a change of variables, which increases the precision in the reaction zone. It transforms the physical coordinate x in a coordinate x' on the uniform mesh ranging from $-\pi$ to π (y being unchanged) by the formula

$$x' = \pi \frac{x/a}{\sqrt{1 + (b-1)\tanh((x/c)^2) + (x/a)^2}}$$

where $b = (a_i/a)^2$ and a, a_i, c are parameters controlling the position of the points in physical space. The meaning of these parameters is given in Denet and Haldenwang (1992). To sum up, for x small, the change of variable is controlled by a: the smaller the a, the more adapted the mesh near 0; for x great, the change of variable is controlled by a_i, the greater a_i, the more distant the points from $x = 0$. The change from one behavior to the other occurs around $x = c$.

In our numerical measurement of growth rates, we take, e.g. for $\beta = 10$, 149 points in the x direction, $a = 5$, $a_i = 20$, $c = 8.5$. When β increases, we reduce a in order to adequately resolve the reaction zone, which is smaller when b is great, while keeping the same value for the other parameters a_i and c, and adding a few points.

5.2 Results

The theoretical dispersion relation depends on the parameters G, γ, and of β and Le through $l = \beta (Le - 1)$. We will vary these parameters, and also the shear viscosity μ.

Variation with Zeldovich number. In Denet and Haldenwang (1992), it was found that the numerical dispersion relation in the case of the diffusive-thermal instability depended a lot on β, at constant l. The first question we ask is whether the situation is similar in the Darrieus-Landau case. We will note σ_{num}, the growth rates values obtained numerically, and σ_{th}, the Pelcé-Clavin theoretical values, (given in a previous section).

In Table I, we vary β for constant $l(l = 0)$ with the other parameters fixed at $\gamma = 0.8$, $G = 0$ and $\mu = 0.7$ and for $k = 0.20944$ (corresponding to a wavelength of 30 in units of flame thickness). It can be seen that the observed growth rates are practically constant for all values of the Zeldovich number, the differences being probably smaller than the typical error we make.

Table II is the same as Table I except that we take now $l = -1$, all the other parameters having the same value as before. In this case too, the differences are very small between different β.

TABLE I

Numerical growth rates vs. Zeldovich number for $k = 0.20944$
$l = 0$ $G = 0$ $\mu = 0.7$ $\gamma = 0.8$ ($\sigma_{th} = 4.3 \times 10^{-2}$)

β	σ_{num}
10	8.13×10^{-2}
15	8.13×10^{-2}
20	8.20×10^{-2}

TABLE II

Numerical growth rates vs. Zeldovich number for $k = 0.20944$
$l = -1\ G = 0\ \mu = 0.7\ \gamma = 0.8\ (\sigma_{th} = 1.11 \times 10^{-1})$

β	σ_{num}
10	1.43×10^{-1}
15	1.40×10^{-1}
20	1.39×10^{-1}

We conclude that, contrary to the diffusive thermal instability, here the effect of Zeldovich number is very small. As a consequence, we will not vary this parameter any further. Note that we disagree on this point with Fröhlich and Peyret (1991), who conclude that the variation with β is important. We actually agree with their values for relatively low values of β (up to $\beta = 10$), the disagreement being limited to higher Zeldovich numbers. Explanation for this disagreement seems to be that they use the same mesh for all values of β, instead of adding precision in the reaction zone, when β increases.

The differences in sensitivity in the Zeldovich number between Darrieus-Landau and thermal-diffusive instabilities can be understood in the following way. For the thermal-diffusive case, the leading order in k, and all the following terms of the dispersion relation contain β, i.e. depend on the flame structure. On the contrary, in the Darrieus-Landau case, we have seen that the leading order in k depends only on γ: thus the flame structure has absolutely no effect on this leading term in k. The variation with β, at constant l, of the dispersion relation only occurs as a correction to the next terms of the k expansion. Furthermore, contrary to the diffusive thermal case, the k^2 terms do not depend only of the Markstein length (i.e. of the flame structure), but also of gas expansion. So in the case of the hydrodynamic instability, only the k^2 term (the second term in this case) is partly dependent on β; on the contrary, in the case of the thermal-diffusive instability the first term (the k^2 term in this case) depends in an important way on β. Thus the β dependence seems to have no important effect in the interesting range of wavenumbers. Note, however, that the numerical measurements we have made concerning the β dependence have been performed for Lewis numbers close to one, which is rather realistic, and wave vectors close to the maximum growth rate. It could be that for lower Lewis numbers and higher wave vectors, the β dependence is more important. However, the quantitative agreement between asymptotics and numerics for values of β not too high shows that the range of applicability of activation energy asymptotics is very large in this hydrodynamic problem.

In the sequel, we will keep the Zeldovich number constant and will always take $\beta = 10$.

Variation with shear viscosity. There is no variation of the theoretical dispersion relation with shear viscosity. This dispersion relation being valid up to terms of order k^2, it means that the effect of viscosity can be seen only on terms of order k^3.

In Table III, we compare the numerical values of growth rates for two values of shear viscosity, for $\beta = 10$, $Le = 1$, $G = 0$, $\gamma = 0.8$ and $k = 0.20944$. The difference, although

TABLE III

Numerical growth rates vs. shear viscosity for $k = 0.20944$ $\beta = 10$
$Le = 1$ $G = 0$ $\gamma = 0.8$ ($\sigma_{th} = 4.3 \times 10^{-2}$)

μ	σ_{num}
0.7	8.13×10^{-2}
0.2	7.87×10^{-2}

not negligible, is small, in agreement with theory. As a consequence, we will take $\mu = 0.7$ for all other computations of growth rates.

Variation with Lewis number. We vary now the Lewis number, at constant β, which is the same as varying $l = \beta(Le - 1)$ at constant β. We take $\beta = 10$, $G = 0$, $\gamma = 0.8$, $\mu = 0.7$. Recall that the theory must be valid for sufficiently low k.

In Figure 1, we plot the numerical, the Pelcé-Clavin and the Darrieus-Landau growth rate, versus the wave vector for $Le = 1$. There is indeed a very good agreement between numerics and the Pelcé-Clavin results for $k < 0.1$; above this value the agreement, although not extremely bad, deteriorates. We give in Table IV the coefficients of a fit of the numerical and Pelcé-Clavin curves by polynomials of the fifth order in k. To fit these two curves, we use in both cases only a few points. The analytical coefficients of a development in powers of k of the Pelcé-Clavin dispersion relation are
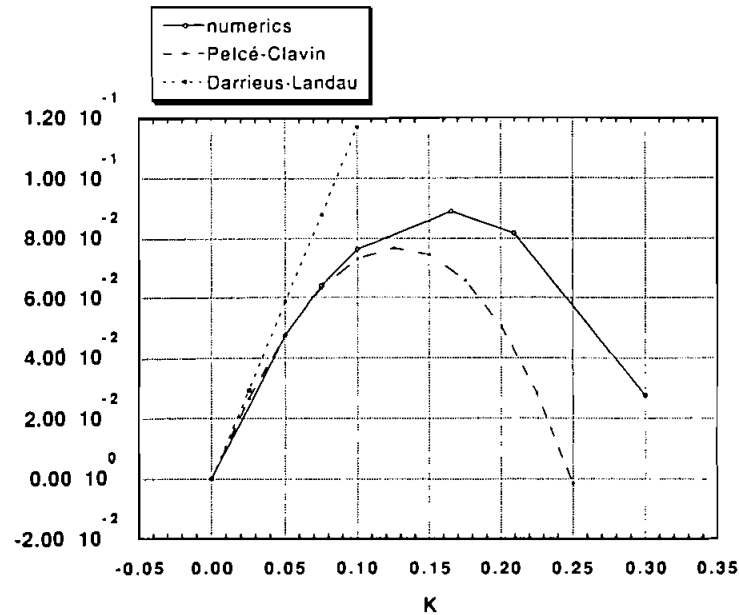

FIGURE 1   Growth rates vs. wave vector for $\beta = 10$ $Le = 1$ $G = 0$ $\mu = 0.7$ $\gamma = 0.8$: numerical dispersion relation (continuous line), Darrieus-Landau dispersion relation (dotted line), Pelcé-Clavin dispersion relation (dashed line).

TABLE IV

Coefficients of a least-square fit of the Pelcé-Clavin and numerical dispersion relations by a fifth-order polynomial for $\beta = 10$ $Le = 1$ $G = 0$ $\gamma = 0.8$ $\mu = 0.7$ $s = a_0 + a_1 k + a_2 k^2 + a_3 k^3 + a_4 k^4 + a_5 k^5$ (the theoretical values are $a_0 = 0$ $a_1 = 1.17$ $a_2 = -4.32$)

	Numerics	Pelcé-Clavin
a_0	1.3×10^{-6}	3.9×10^{-7}
a_1	1.16	1.17
a_2	-4.54	-4.19
a_3	7.94	-2.61
a_4	-24.2	6.88
a_5	28.8	-18.70

also given. Comparison of these analytical coefficients with the results of the fit of the theoretical curve illustrates the typical error in this fit. The coefficients are approximately the same up to the order two, and the Pelcé-Clavin dispersion relation is precisely valid up to terms of order k^2, so that the agreement is excellent, specially with a very few number of points. This agreement clearly validates the numerical scheme, we have used, and shows that the difference between theory and numerics is thus caused essentially by terms of order k^3.

Figure 2 is the same as Figure 1, except that $Le = 0.75$ ($l = -2.5$). Diffusive effects are less stabilizing in this case, and the numerical curve is closer to the Darrieus-Landau
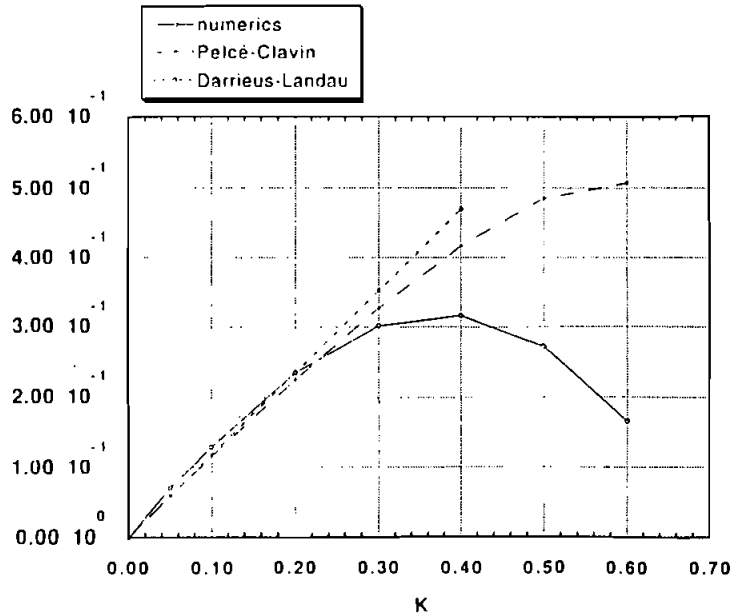

FIGURE 2   Growth rates vs. wave vector for $\beta = 10$ $Le = 0.75$ $G = 0$ $\mu = 0.7$ $\gamma = 0.8$: numerical dispersion relation (continuous line), Darrieus-Landau dispersion relation (dotted line), Pelcé-Clavin dispersion relation (dashed line).

curve. As a consequence, there is good agreement on a wider range than before (up to $k = 0.3$). But the Pelcé-Clavin dispersion relation is not much better in this case than the Darrieus-Landau one, and the differences between theory and numerics can become extremely great for higher unstable wave vectors. Of course, the unstable, interesting range being wider, there are more chances for an unstable wave vector to get out of the domain of validity of the Pelcé-Clavin relation. Thus it is perfectly natural to observe that discrepancies increase when the Lewis number is reduced; this tendency could be predicted before any actual measurement. The multi-scale method based on the low k approximation just happens not to give good quantitative results in the unstable range of wavenumbers for too low Lewis numbers; it does not mean of course that this multi-scale method is not valid; we have seen previously that it works quite well in the $Le = 1$ case. As before, we present in Table V a fit of these curves by a fifth-order polynomial: the agreement is worse than before, especially concerning the terms of order k^2. Note that the number of points is still small, and it seems difficult to get a good fit of the second order terms, which are small in this case.

In Figure 3, we take $Le = 1.25$ ($l = 2.5$); good agreement between theory and numerics is limited to $k < 0.075$, but, the unstable range being smaller, theoretical and numerical curves are rather close. In Table VI, we give the comparison betwen fits of these two curves: the k^2 terms are nearer in relative value than in the $Le = 0.75$ case, but the agreement on these terms is not very good.

TABLE V

Coefficients of a least-square fit of the Pelcé-Clavin and numerical dispersion relations by a fifth-order polynomial for $\beta = 10\ Le = 0.75\ G = 0\ \gamma = 0.8\ \mu = 0.7$
$s = a_0 + a_1 k + a_2 k^2 + a_3 k^3 + a_4 k^4 + a_5 k^5$ (the theoretical values are $a_0 = 0$
$a_1 = 1.17\ a_2 = -0.36$)

	Numerics	Pelcé-Clavin
a_0	5.5×10^{-4}	5.2×10^{-6}
a_1	1.40	1.16
a_2	-0.89	0.08
a_3	-0.45	-2.01
a_4	-4.33	4.66
a_5	4.04	-5.00

TABLE VI

Coefficients of a least-square fit of the Pelcé-Clavin and numerical dispersion relations by a fifth-order polynomial for $\beta = 10\ Le = 1.25\ G = 0\ \gamma = 0.8\ \mu = 0.7$
$s = a_0 + a_1 k + a_2 k^2 + a_3 k^3 + a_4 k^4 + a_5 k^5$ (the theoretical values are $a_0 = 0$
$a_1 = 1.17\ a_2 = -8.28$)

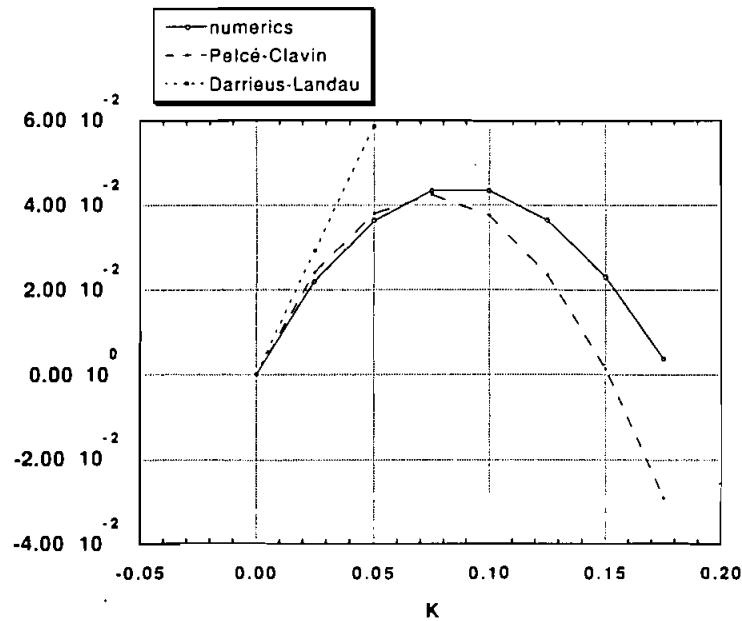|	Numerics	Pelcé-Clavin
a_0	2.3×10^{-6}	1.0×10^{-6}
a_1	1.03	1.18
a_2	-6.15	-8.56
a_3	1.19	7.14
a_4	4.98	-20.2
a_5	1.90	49.3

FIGURE 3   Growth rates vs. wave vector for $\beta = 10$ $Le = 1.25$ $G = 0$ $\mu = 0.7$ $\gamma = 0.8$: numerical dispersion relation (continuous line), Darrieus-Landau dispersion relation (dotted line), Pelcé-Clavin dispersion relation (dashed line).

Variation with gravity.   We will take $\beta = 10$, $Le = 1$, $\gamma = 0.8$, $\mu = 0.7$ and vary G, the inverse of the Froude number. The case $G = 0$ has been examined in Figure 1. $G > 0$ corresponds to downward propagating flames and $G < 0$ to upward propagating flames.

In Figure 4, we take $G = 0.3$. This case is chosen in order to be close to the theoretical stability limit. Secondary instabilities of downward propagating flames, like this case, are studied in Denet (1993), but here we are only interested in linear results. We plot the numerical and Pelcé-Clavin dispersion relations. In this case, there is still a good agreement for low k (< 0.1), but the differences are extremely great, both on the value of the maximum of the curve, and on the width of the unstable range of wave vectors. These differences just show that the terms neglected in the expansion in powers of k slightly shift the threshold of Darrieus-Landau instability, resulting in a high relative error (compared to numerics) for values of G close to this threshold. However, the differences in absolute value are of the same order as those found for $G = 0$.

In Figure 5, we take $G = -0.3$. As before, the two curves, theoretical and numerical, are very close for sufficiently low k.

In these two cases of non-vanishing G, the additional theoretical hypothesis $G = O(\varepsilon) = O(k)$ does not seem to diminish the agreement for low k (but we have not used very low values of k).

Variation with gas expansion.   In the previous paragraph, we examined the case $G = 0.3$ (Fig. 4), showing that the theoretical predictions are not very good in the vicinity of the stability limit. This result seems to contradict the conclusion of Jackson and Kapila (1986) (see also Jackson and Kapila, 1984), who concluded to
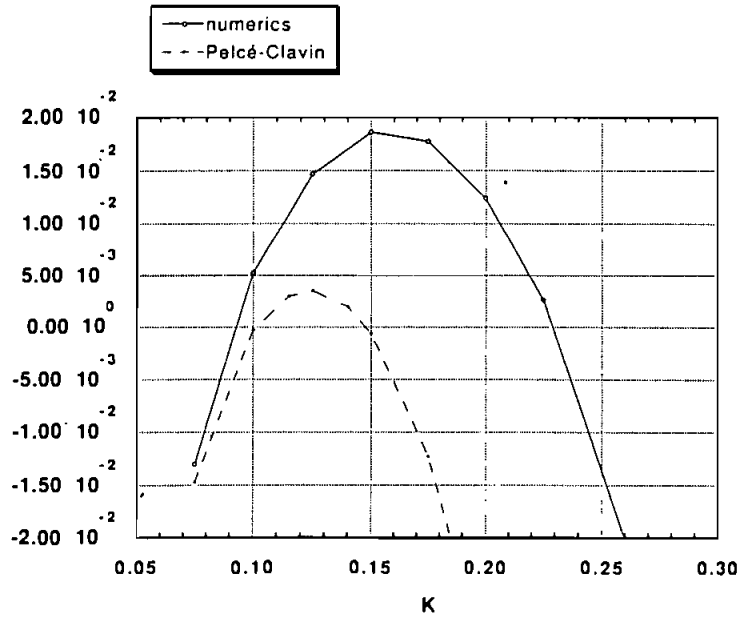
FIGURE 4   Growth rates vs. wave vector for $\beta = 10$ $Le = 1$ $G = 0.3$ $\mu = 0.7$ $\gamma = 0.8$: numerical dispersion relation (continuous line), Pelcé-Clavin dispersion relation (dashed line).
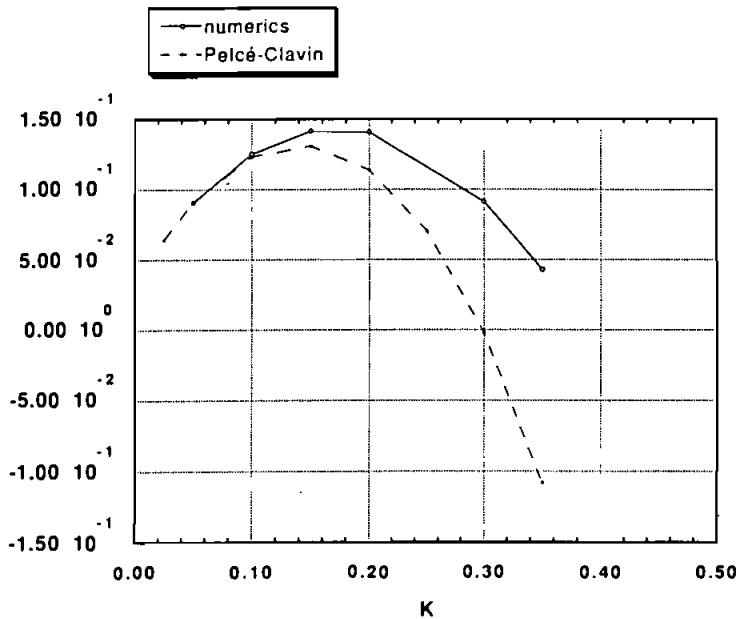

FIGURE 5   Growth rates vs. wave vector for $\beta = 10$ $Le = 1$ $G = -0.3$ $\mu = 0.7$ $\gamma = 0.8$: numerical dispersion relation (continuous line), Pelcé-Clavin dispersion relation (dashed line).

a good agreement with theory on the width of the unstable band. These authors were using a mixed numerical-theoretical method, as explained in the introduction, and did not compute growth rates. It can be noted that the disagreement is more important on the growth rate values than on the unstable band width. However, it seems that there is some discrepancy remaining between our results and those of Jackson and Kapila.

The conclusion of these authors is based on a figure in which they take $y = 0.5$ (i.e. the temperature grows from 1 to 2 in physical units), a low value compared to our $y = 0.8$ (i.e. the temperature grows from 1 to 5 in physical units). The value $y = 0.8$ is more typical of experiments and is often used in numerical simulations (see Peters and Warnatz, 1982).

Fröhlich and Peyret (1991) found that for $G = 0$ and near the maximum of the dispersion relation, the agreement was better for lower y. In Figure 6, we take $y = 0.66$, $\beta = 10$, $Le = 1$ and $G = 0.16$ to be, as in Figure 4, close to the stability limit. We choose the same scales as in Figure 4; it can be seen that the agreement is better in Figure 6, both for the position of the maximum and for the width of the unstable band. This effect seems to explain the discrepancies between Jackson.and Kapila's and our results. Curiously, the agreement is worse for low k in Figure 6 than in Figure 4.

6 NUMERICAL SIMULATIONS OF LARGE AMPLITUDE FLAMES

In this section, we will calculate stationary solutions, with constant parameters $\beta = 10$, $Le = 0.9$, $y = 0.8$. The computations of this section are much more time-consuming

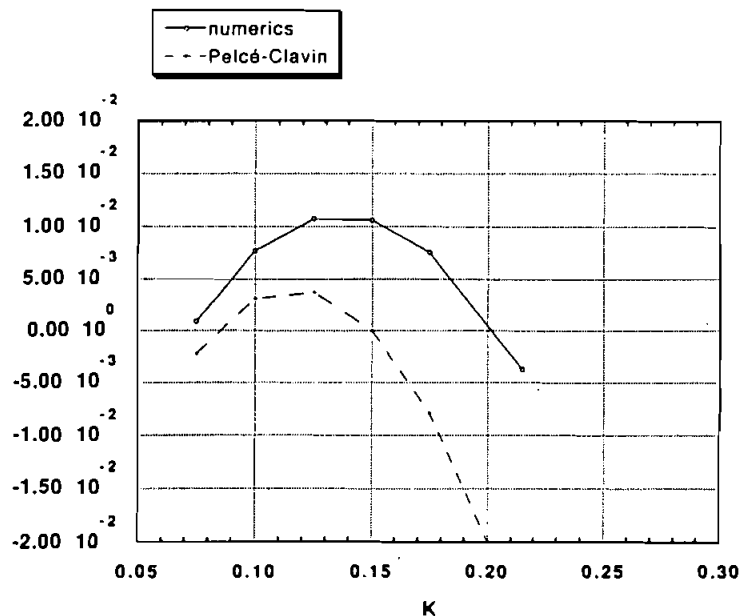FIGURE 6   Growth rates vs. wave vector for $\beta = 10$ $Le = 1$ $G = 0.16$ $\mu = 0.7$ $y = 0.66$: numerical dispersion relation (continuous line), Pelcé-Clavin dispersion relation (dashed line).

than simply calculating growth rates, as in section 5, and we will limit ourselves to a few cases. We take as initial condition a sinusoidal flame. The flame is considered as stationary when the residual that we defined by

$$\frac{1}{\Delta t}\frac{1}{N_x N_y}\sum_{i=1}^{N_x}\sum_{j=1}^{N_y}|T_{ij}^{n+1} - T_{ij}^n|$$

is smaller than 10^{-5}. Δt is the time step, $n + 1$ represents the new time step, n the last time step, N_x and N_y are the number of points respectively in the x and y directions.

We have previously mentioned that we could use a self-adaptive mesh in the x direction. In fact, we have problems with such techniques, because adapting the mesh means losing some information in interpolating the variables, and unfortunately curved flames are very sensitive to noise (see Zeldovich et al., 1980). Variations of the flame amplitude are produced by the interpolation, and we need again adapting the mesh and interpolating. Similar effects have been observed by Denet and Larrouturou (1988).

To overcome these effects, we are obliged to use a uniform mesh, with a high number of points in the x direction. We use 120 points in the x direction and 32 modes in the y direction. After a stationary solution has been obtained, we can adapt the mesh and obtain a stationary solution on the adapted mesh, of the same amplitude as the solution on the uniform mesh, showing that this solution is a good one. But we did not succeed in adapting the mesh in the course of the calculation.

Curved flame produced by the Darrieus-Landau instability. We take a rectangular domain: width 20 (in the y direction), length 30 (in the x direction). The gravity parameter is $G = 0$ (pure Darrieus-Landau case) and $\mu = 0.7$.

The temperature lines of the stationary solution are plotted in Figure 7a, the streamlines in Figure 7b, and the vorticity lines in Figure 7c. The values of the
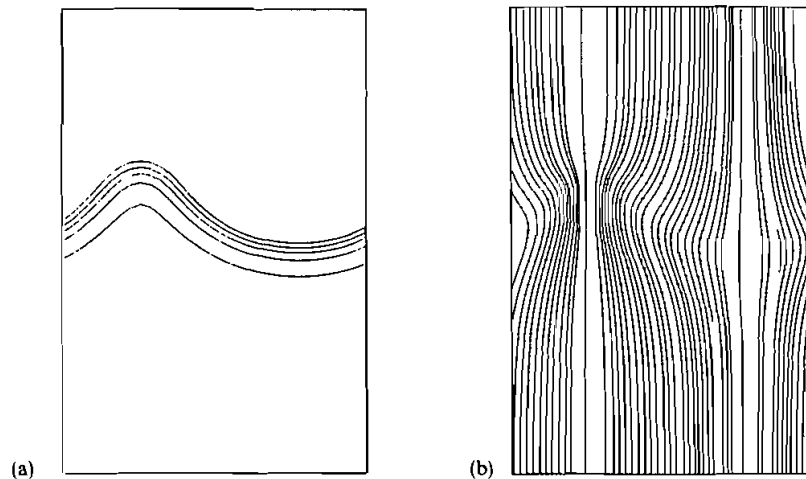

(a)   (b)

FIGURE 7   Stationary flame for $\beta = 10$ $Le = 0.9$ $G = 0$ $\mu = 0.7$ $\gamma = 0.8$: temperature lines (Fig. 7a), stream-lines (Fig. 7b), vorticity lines (Fig. 7c), shear amplitude vs. x (Fig. 7d), v_x vs. y for $x = 30$ (Fig. 7e).
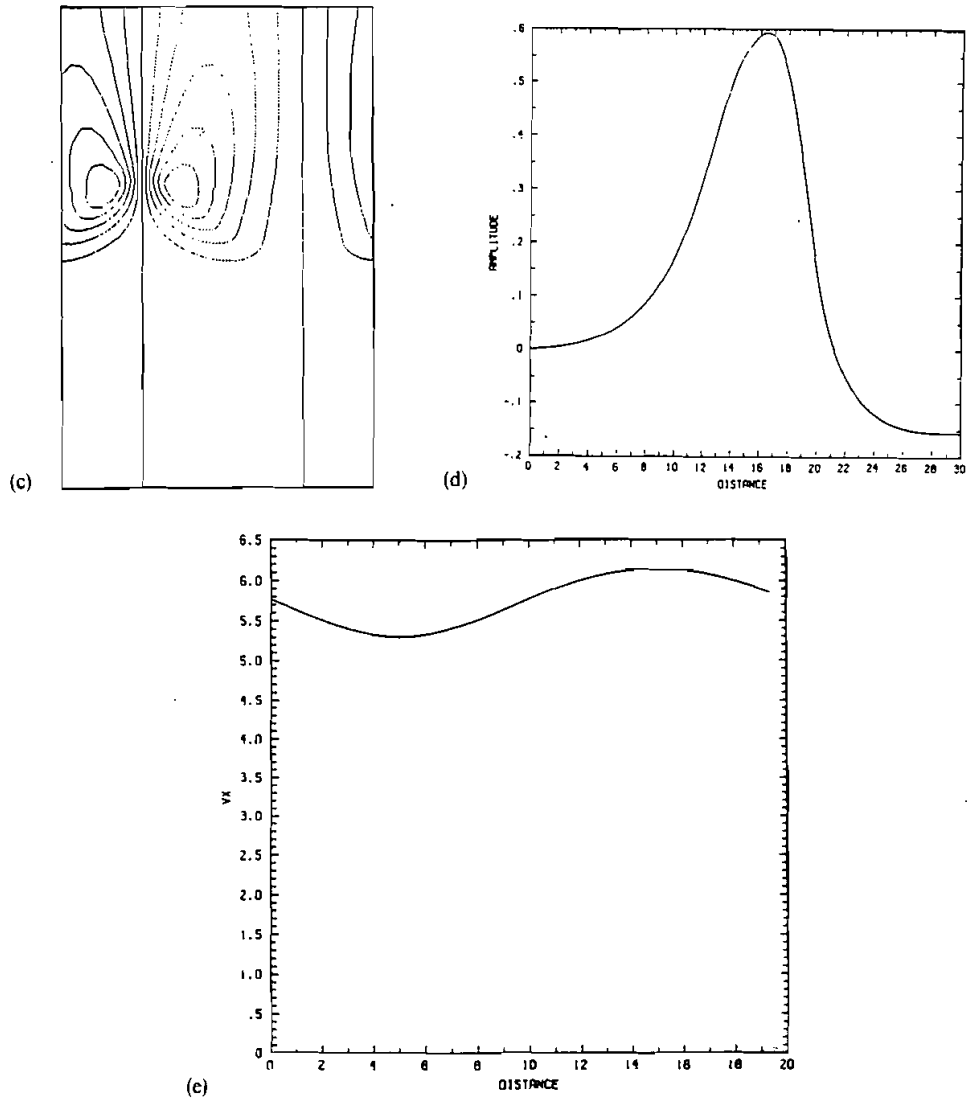
(c)

(d)

(e)

FIGURE 7   (Continued.)

temperature drawn are $T = 0.1, 0.3, 0.5, 0.7$ and 0.9. The same values will also be used in the next figures of temperature lines. The solution has only one cell, with a cusp typical of hydrodynamic instability pointing towards burnt gases. The deflection of stream-lines (due to conservation of normal mass flux and transverse velocity) across the flame front is easily seen. Because the flame is unstable with respect to the Darrieus-Landau instability, the streamlines converge when going from the fresh gases to the cusp. As a consequence of this deflection of streamlines, vorticity, which was very small in the fresh gases, is created behind the flame front, i.e. in the burnt gases. This effect is

clear in Figure 7c, where lines, corresponding to equidistant values of vorticity, are plotted: the variation being essentially located in the burnt gases, and in the flame itself.

Let us define ampli (x) the amplitude of shear for a fixed value of x as

$$\text{ampli}(x) = \rho\, v_x(x, y_1) - \rho\, v_x(x, y_2)$$

where y_1 is the value of y corresponding to the location of the "cusp" pointing towards burnt gases, and y_2 corresponds to the location of the "tip" pointing towards fresh gases. We have chosen to include the density in this definition, to discard effects due to the big variation of the velocity, when crossing the flame front. This definition of amplitude of shear will also be used in the next paragraph, concerned with stable flames submitted to a shear flow.

In Figure 7d, this amplitude of shear is plotted vs. x, showing first an increase (to reach a maximum approximately at the flame location), and then a violent decrease, the amplitude becoming negative at the end of the domain. The increase is caused by the convergence of streamlines in the fresh gases. On the contrary, the divergence of streamlines, just behind the flame, explains the decrease.

In Figure 7f, we show the result of all these hydrodynamical effects at the end of the domain, i.e. the longitudinal velocity vs. y at this position: the velocity is minimum for the value of y corresponding to the cusp. Of course, because of viscosity effects, this shear created by the flame will decay far in the burnt gases, but our domain is not very long.

Stable flames submitted to a shear flow. The flame is submitted to a shear flow, i.e. we use as boundary conditions for v_x.

$$v_x(-X_0) = U + a \sin(k y).$$

In the case of a stable downward propagating flame, this problem has been studied theoretically by Searby and Clavin (1986), and experiments are reported in Searby *et al.* (1983). Strictly speaking, the theory is only valid for low amplitude flames. Here, we choose to obtain large amplitudes; nevertheless, the theory will be useful to explain qualitative aspects of our results. We will use a square domain: width and length are equal to 30 (in units of flame thickness).

In Figure 8, we show the temperature lines and the streamlines in the case of a very stable flame $a = 0.2$, $G = 0.75$ and $\mu = 0.7$. The final solution is a sinusoidal flame. Because the flame is stable, the streamlines diverge when going from the fresh gases to the cusp, contrary to Figure 7. Unfortunately, a quantitative numerical study of this problem would be very expensive. So, we will content ourselves with a qualitative description of the flow induced by the flame. The vorticity lines, corresponding as before to equidistant values, are shown in Figure 8c. Just as in the case of the unstable flame reported before (although the maximum and minimum values are different), the main variation of vorticity is located in the flame and in the burnt gases.

In Figure 8d, we have the amplitude of shear (defined in the previous paragraph) versus x. Here, the shear is not zero in the fresh gases, and, because $a = 0.2$, we start from an amplitude of 0.4. As a consequence of streamlines divergence, this amplitude decreases,then becomes negative near the flame. As before, viscosity effects should take place far in the burnt gases, reducing slowly the amplitude of shear to zero.
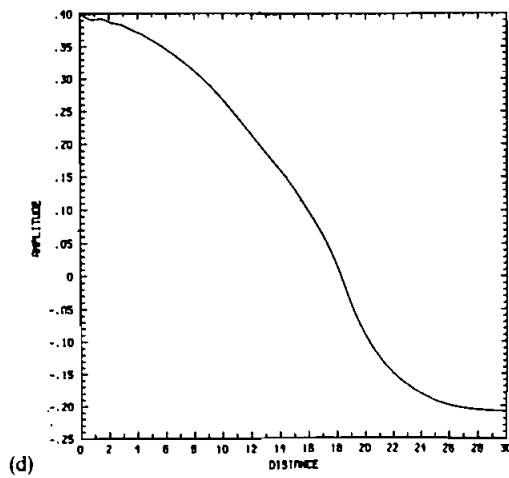
(a)

(b)

(c)
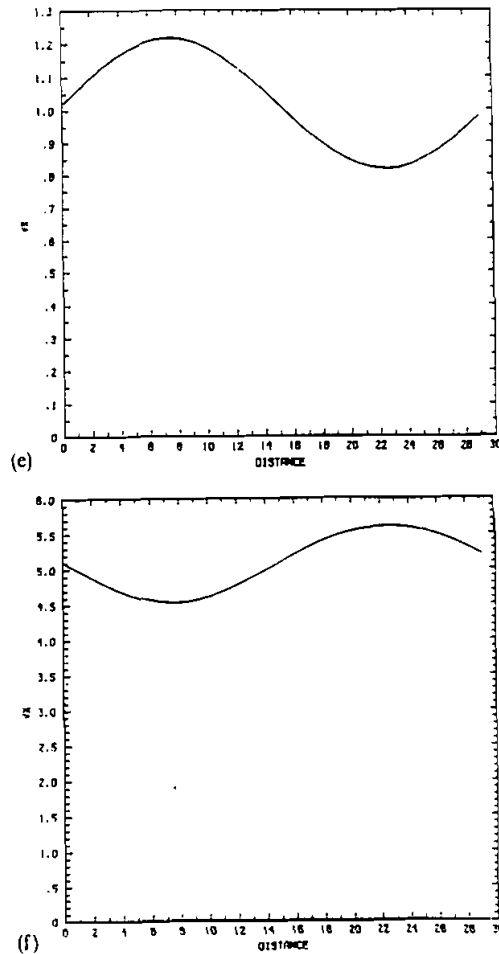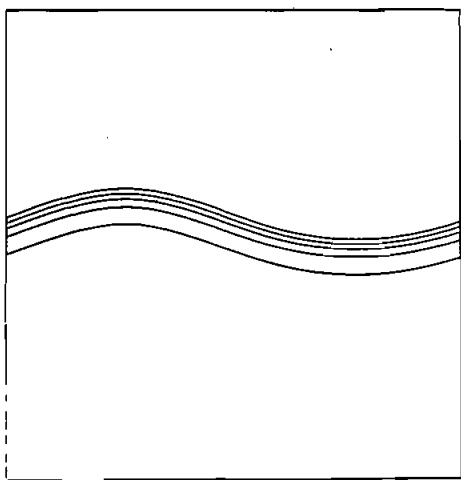
(d)

(e)

(f)
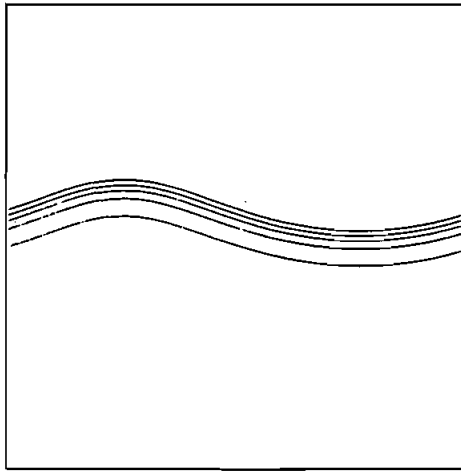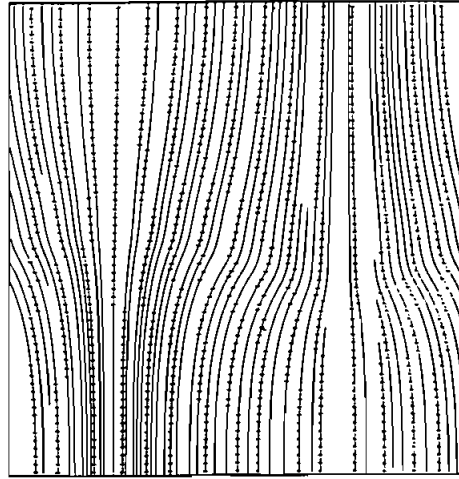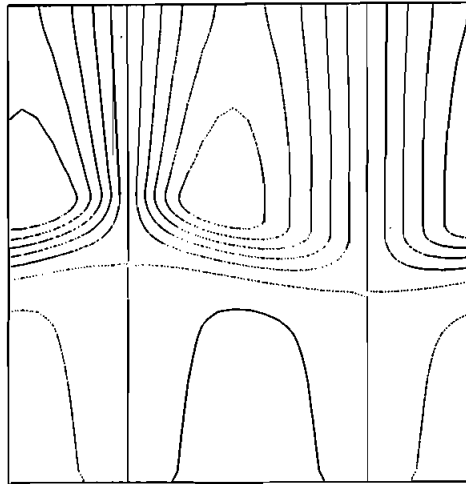
FIGURE 8   Stationary flame for $\beta = 10$ $Le = 0.9$ $G = 0.75$ $\mu = 0.7$ $\gamma = 0.8$ $a = 0.2$: temperature lines (Fig. 8a), streamlines (Fig. 8b), vorticity lines (Fig. 8c), shear amplitude vs. x (Fig. 8d), v_x vs. y for $x = 0$ (Fig. 8e), v_x vs. y for $x = 30$ (Fig. 8f).

This inversion effect is actually predicted by the theory of Searby and Clavin (1986). This effect is clearly exhibited in Figures 8e and 8f showing the longitudinal velocity vs. y respectively at the beginning $(x = 0)$ and the end $(x = 30)$ of the domain.

In Figure 9, we show the effect of viscosity by taking $\mu = 0.2$ instead of $\mu = 0.7$ in Figure 8, all the other parameters being equal in both cases. It is difficult to see differences between Figures 8 and 9 from the point of view of temperature lines: the amplitude, as predicted by Searby and Clavin (1986), is independent of viscosity if the viscosity does not depend on temperature, which is the case here).
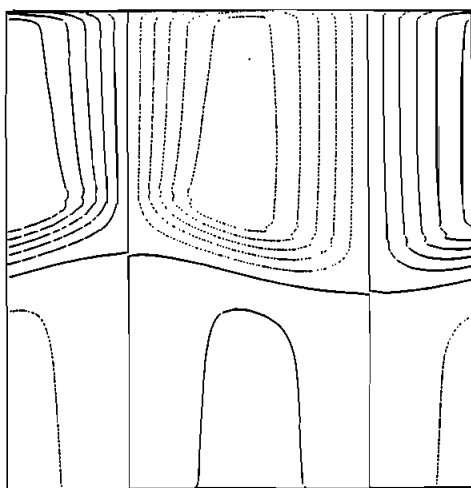
On the contrary, as shown by the comparison between Figures 9b and 8b, the flow, at least in the flame and in the burnt gases, depends a little on viscosity. Once again, it does not contradict the theoretical predictions. Vorticity lines are plotted in Figure 9c,
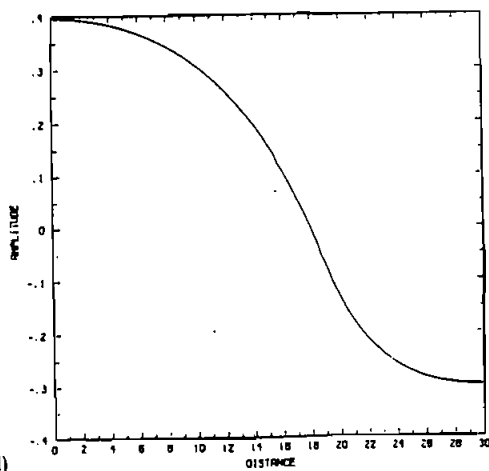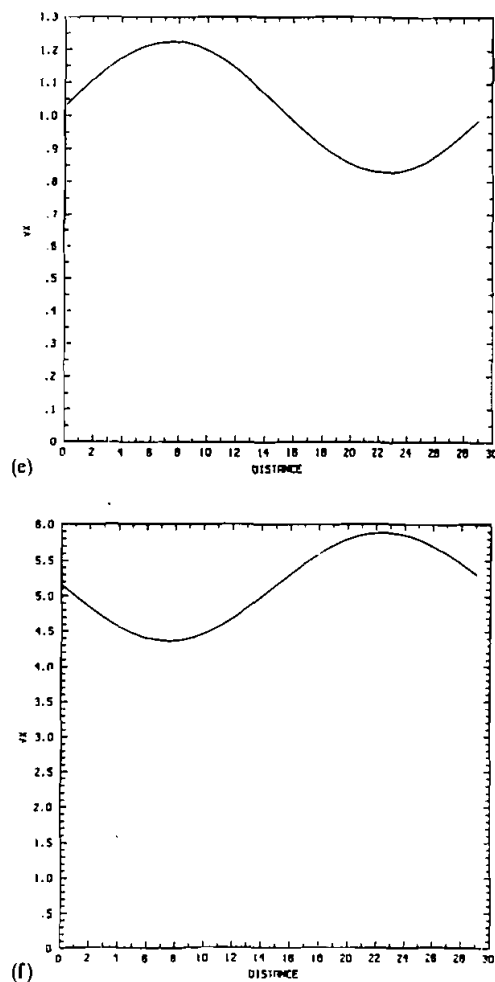
(a)

(b)

(c)

(d)

(e)

(f)
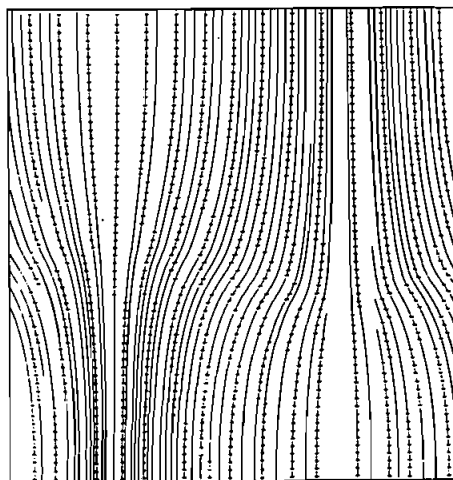
FIGURE 9 Stationary flame for $\beta = 10$ $Le = 0.9$ $G = 0.75$ $\mu = 0.2$ $\gamma = 0.8$ $a = 0.2$: temperature lines (Fig. 9a), streamlines (Fig. 9b), vorticity lines (Fig. 9c), shear amplitude vs. x (Fig. 9d), v_x vs. y for $x = 0$ (Fig. 9e), v_x vs. y for $x = 30$ (Fig. 9f).

amplitude of shear on Figure 9d (it does not decrease exactly to the same value as in Fig. 8d). In Figures 9e and 9f, we have the longitudinal velocity vs. y at the beginning and the end of the domain.

7 CONCLUSION

In this work we were interested in the Darrieus-Landau instability of plane premixed flames, a phenomenon of hydrodynamical nature caused by the density jump across the

flame. We have introduced a numerical algorithm based on a momentum pressure formulation that was designed to handle the problem of isobaric hydrodynamics with variable density that is characteristic of premixed flames. With this algorithm, it was possible to measure numerically the growth rates of the Darrieus-Landau instability for finite values of the Zeldovich number β (reduced activation energy) and to compare them with theoretical predictions valid when:

(i) the Zeldovich number is large (high activation energy asymptotics), and
(ii) the wavenumber is small (multi-scale method).

It was found that the results for the values of growth rates do not depend very much on the value of β, at constant $l = \beta(Le - 1)$, showing that activation energy asymptotics works well in this problem even for values of β close to 10, i.e. not extremely large, unlike a previous study we have made of the thermodiffusive instability (Denet and Haldenwang, 1992). On the contrary, the second limit of small wavenumber caused some discrepancies between theory and numerical measurements when the unstable band of wavenumber gets large, i.e. in the case of low Lewis numbers, corresponding to small values of Markstein length. However, for a Lewis number unity, a close agreement between theory and numerics was found. Variations of the computed growth rates with viscosity and gravity were also presented, showing that the growth rates depend very slightly on the viscosity, in accordance with theoretical predictions, and that the measured threshold of instability of the plane flame is slightly displaced compared to the low wavenumber prediction.

Simulations of finite amplitude flames were presented, showing very clearly the deflection of streamlines across the flame which is the main cause of the Darrieus-Landau instability. Stable flames excited by a stationary shear flow were also simulated at the end of the paper; in this case, the retroaction of the flame on the flow field is so important that the shear flow gets inverted in the burnt gases compared to its fresh gases value.

REFERENCES

Barenblatt, G. I., Zeldovich, Y. B. and Istratov, A. G. (1962). On diffusional thermal stability of laminar flames, *Prikl. Mekh. Tekh. Fiz.* **2**, 21.
Clavin, P. (1985). Dynamic behaviour of premixed flame fronts in laminar and turbulent flows, *Prog. Energy Combust. Sci.*, **11**, 1–59.
Clavin, P. and Williams, F. A. (1982). Effects of molecular diffusion and of thermal expansion on the structure and dynamics of premixed flames in turbulent flows of large scale and low intensity, *J. Fluid Mech.*, **116**, 251.
Darrieus, G. (1938). Propagation d'un front de flamme, communication presented at La Technique Moderne.
Denet, B. (1988). Thesis, Université de Provence, Marseille.
Denet, B. (1993). On nonlinear instabilities of cellular premixed flames, *Combust. Sci. Tech.*, **92**, 123.
Denet, B. and Haldenwang, P. (1992). Numerical study of thermal diffusive instability of premixed flames, *Combust. Sci. Tech.*, **86**, 199.
Denet, B. and Larrouturou, B. (1988). Private communication.

Frankel, M. I. and Sivashinsky, G. I. (1983). The effect of viscosity on hydrodynamic stability of a plane front, *Combust. Sci. Tech.*, **31**, 131.

Fröhlich, J. and Peyret, R. (1991). A spectral algorithm for low Mach number combustion, *Comp. Meth. in applied Mech. and Engineering*, **90**, (1/3), 631.

Gottlieb D. und Oryzag S. A. (1977). Numerical analysis of spectral methods. SIAM Philadelphia.

Jackson, T. L. and Kapila, A. K. (1984). Effect of thermal expansion on the stability of plane, freely propagating flames, *Combust. Sci. Tech.*, **41**, 191.

Jackson, T. L. and Kapila, A. K. (1986). Effect of thermal expansion on the stability of plane, freely propagating flames part II: incorporation of gravity and heat loss, *Combust. Sci. Tech.*, **49**, 305.

Landau, L. (1944). On the theory of slow combustion, *Acta Physicochim. URSS*, **19**, 77.

Linan, A. (1990). Private communication.

Majda, A. and Sethian, J. (1985). The derivation and numerical solution of the equations for zero Mach number combustion, *Combust. Sci. Tech.*, **42**, 185.

Matalon, M. and Matkowsky, B. J. (1982). *J. Fluid Mech.*, **124**, 239.

Pelcé, P. and Clavin, P. (1982). The influence of hydrodynamics and diffusion upon the stability limits of laminar premixed flames, *J. Fluid Mech.*, **124**, 219.

Peters, N. and Warnatz, J. Ed. (1982). *Notes in numerical fluid mechanics 6*, Vieweg.

Quinard, J., Searby, G. and Boyer, L. (1984). Cellular structures of premixed flames in uniform laminar flow, In *Cellular structures in instabilities*, Lecture Notes in Physics, Weisfreid J. E. and Zaleski S. Ed., Springer Verlag, **210**, 331–341.

Roache, P. J. (1972). *Computational fluid dynamics*, Hermosa.

Searby, G., Sabathier, F., Clavin, P. and Boyer, L. (1983). The hydrodynamical coupling between the motion of a flame and the upstream gas flow, *Phys. Rev., Lett.*, **51**, 1450.

Searby, G. and Clavin, P. (1986). Weakly turbulent wrinkled flames in premixed gases, *Combust. Sci. Tech.*, **46**, 167.

Sivashinsky, G. I. (1983). Instabilities, pattern formation and turbulence in flames, *Ann. Rev. Fluid Mech.*, **15**, 179–199.

Spalding, D. B. and Wu, J. Z. Y. (1986). *Phys. Chem. Hydrodynamics*, **7**(5/6), 353.

Williams, F. A. (1985). *Combustion Theory*, The Benjamin/Cummings Publishing Company.

Zel'dovitch, Y. B., Istratov, A. G., Kidin, N. I. and Librovitch, V. B. (1980). Flame propagation in tubes: hydrodynamics and stability, *Combust. Sci. Tech.*, **24**, 1–13.